

---

# DAIN: Dynamic Agent-Based Interaction Network for Efficient and Collaborative Multimodal Reasoning

---

Xinxin Chen Yuchen Li Zihan Wang  
Haoyu Zhang Ruixin Liu Mingyuan Zhao  
University of Chinese Academy of Sciences

## Abstract

Current multimodal fusion approaches, particularly those based on static Mixture-of-Experts (MoE) architectures, often struggle to provide the adaptive and efficient collaborative reasoning required by complex real-world applications. We introduce the Dynamic Agent-based Interaction Network (DAIN), which reconceptualizes multimodal fusion as a dynamic, multi-agent collaborative process. DAIN employs a context-aware Meta-Controller that dynamically schedules sparse activation of specialized interaction agents and orchestrates compressed inter-agent communication for consensus-building. The framework is guided by a multi-objective loss function that jointly optimizes task accuracy, agent specialization, and operational efficiency through sparse activation and communication regularization. Comprehensive evaluations across five diverse benchmarks—ADNI, MIMIC-IV, MM-IMDB, CMU-MOSI, and ENRICO—establish DAIN as a new state-of-the-art, delivering significant performance improvements including a 2.6% accuracy gain on ADNI. Ablation studies verify the critical roles of both dynamic scheduling and agent communication. Furthermore, DAIN offers enhanced interpretability by exposing context-dependent agent roles and collaboration patterns while maintaining computational efficiency through sample-wise sparse agent activation. Our work demonstrates the promise of dynamic, agent-based paradigms for multimodal reasoning.

## 1 Introduction

Effective integration of complementary information from distinct data sources—such as images, text, and audio—remains a fundamental challenge in multimodal machine learning. This integration is particularly critical in domains like healthcare, where accurate diagnostics often depend on synthesizing heterogeneous data streams including medical imaging, clinical notes, and laboratory results. The Partial Information Decomposition (PID) framework [34] provides a principled theoretical lens for analyzing multimodal interactions, decomposing information into uniqueness (modality-specific contributions), redundancy (shared information), and synergy (emergent properties from combination). While PID establishes a strong theoretical foundation, its integration into practical end-to-end deep learning models remains underexplored, as existing fusion methods largely lack explicit mechanisms to model these distinct interaction types.

Mixture-of-Experts (MoE) architectures [25, 28] offer a promising direction by allocating specialized parameters to different interaction patterns through conditional computation. Recent advances have scaled MoE to unprecedented capacities [48, 14], and several works have adapted this paradigm for multimodal tasks [43, 36, 77]. However, conventional MoE frameworks operate with static, predefined collaboration structures that lack dynamic adaptation and resource-efficient coordination. They aggregate expert outputs without mechanisms to dynamically assemble the most relevant experts or facilitate focused, context-aware information exchange among them.

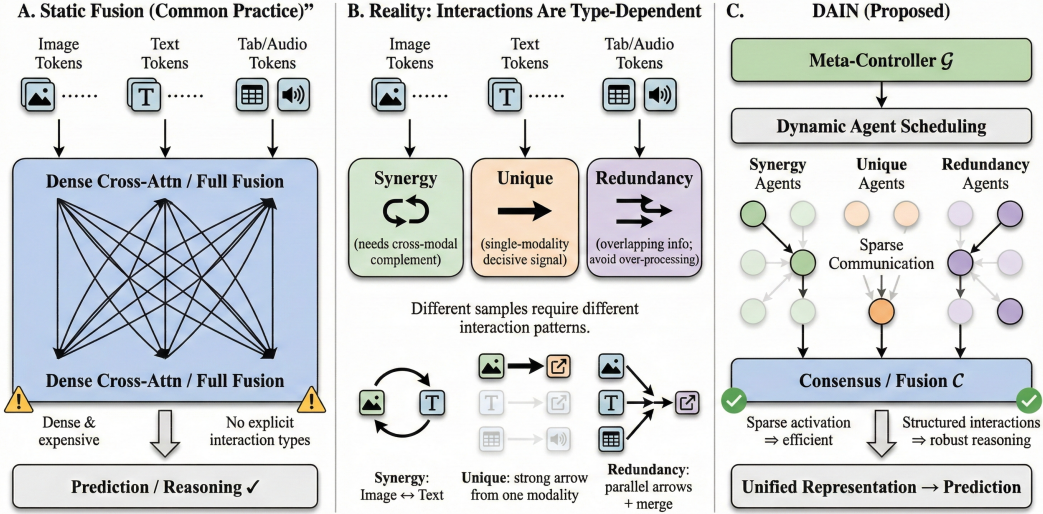


Figure 1: **Motivation.** Static dense multimodal fusion is costly and ignores diverse cross-modal interaction patterns; DAIN models *synergy*, *uniqueness*, and *redundancy* via dynamic, sparse agent collaboration for efficient and robust reasoning.

To address these limitations, we introduce a paradigm shift: we conceptualize multimodal fusion as a collaborative decision-making process among autonomous interaction agents. We propose the Dynamic Agent-based Interaction Network (DAIN), which introduces three key innovations. First, DAIN employs a Meta-Controller that performs context-aware, sparse scheduling of agents, activating only a relevant subset for each input sample. Second, the framework enables structured, compressed inter-agent communication guided by a dynamic graph to efficiently build consensus among active agents. Third, DAIN uses a multi-objective optimization formulation that balances task performance with operational efficiency, promoting sparsity in both agent activation and communication pathways.

This dynamic, agent-based framework is backbone-agnostic and provides structured interpretability through agent activation profiles and communication graphs. Extensive experiments on five diverse multimodal datasets—including two medical benchmarks (ADNI, MIMIC-IV) and three general-purpose benchmarks (MM-IMDB, CMU-MOSI, ENRICO)—demonstrate that DAIN consistently outperforms strong static fusion baselines and prior interaction-aware models (Figure 3). Ablation studies confirm the necessity of both dynamic scheduling and agent communication, while analysis of agent activation patterns reveals interpretable insights about how different interaction types are dynamically recruited for distinct data characteristics.

## 2 Related Work

### 2.1 Multimodal Interaction Theory

The theoretical study of multimodal interactions has been substantially advanced by the Partial Information Decomposition (PID) framework [34], which decomposes information content into uniqueness, redundancy, and synergy components. However, translating these theoretical constructs into end-to-end learning systems remains challenging. Several approaches have attempted to model specific interaction types [83, 29], but these are often limited to particular modality combinations or require separate estimation procedures. Other works focus on interaction quantification [71, 39, 12] but do not provide mechanisms for learning these interactions within unified architectures. Bimodal approaches [72, 13] cannot readily extend to settings with more than two modalities. Our work addresses these gaps by proposing a unified framework that directly models and quantifies diverse interaction types within an end-to-end Mixture-of-Experts architecture.

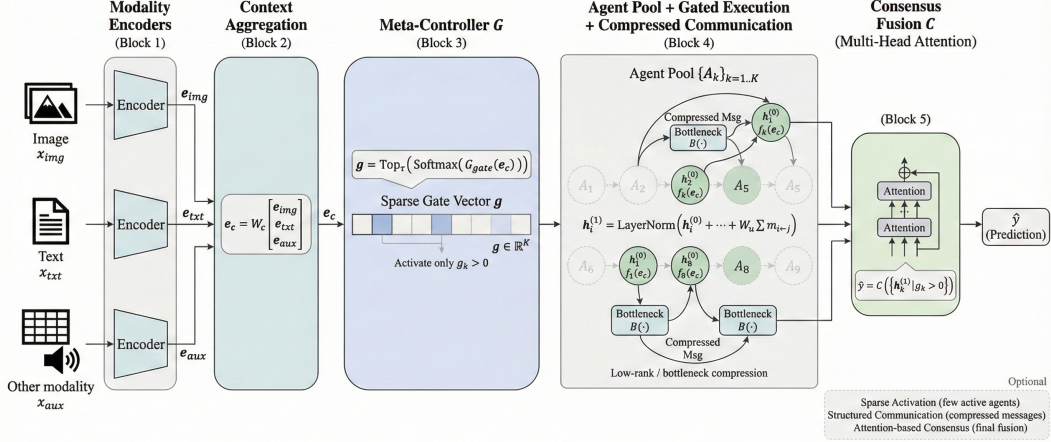


Figure 2: **DAIN architecture.** Encoded multimodal features form a context vector for a meta-controller that sparsely schedules interaction agents; active agents exchange compressed messages and are aggregated by an attention-based consensus module to produce the final prediction.

## 2.2 Multimodal Fusion Architectures

Multimodal fusion strategies have evolved from simple concatenation of modality representations [38] to sophisticated attention-based mechanisms [58, 74, 26]. The Mixture-of-Experts paradigm [25, 28, 78, 7] enables conditional computation where specialized parameters are activated based on input characteristics. Modern large-scale implementations [48, 14, 81] have demonstrated the scalability of sparse expert activation. Recent adaptations for multimodal learning include LIMoE [43], which applies MoE to vision-language contrastive learning, MoE-LLaVA [36], which integrates MoE into large vision-language models, and comprehensive surveys on multimodal LLMs [33]. The MMoE framework [77] explicitly models different interaction types using specialized experts, though it treats interaction modeling as a separate preprocessing stage rather than an integrated end-to-end learning component. Our DAIN framework advances beyond these approaches by introducing dynamic, context-aware expert scheduling and structured inter-agent communication.[82, 6, 5, 76, 84, 9, 11, 10, 84, 23]

## 2.3 Multimodal Interpretability

Interpretability in multimodal systems aims to explain model decisions and quantify the contribution of different modalities and their interactions. Prior approaches have focused on attention visualization [4, 3] or individual modality attribution [24, 21, 50]. Some methods generate human-readable rationales [45, 80, 8] but do not quantify the relative contribution of interaction types. Others lack structured taxonomies for categorizing interactions [57, 35, 70]. DAIN addresses these limitations by providing interpretability through explicit agent activation profiles and communication graphs, enabling both local (per-sample) and global (dataset-level) analysis of interaction dynamics.[20, 69, 32, 47]

# 3 Method

## 3.1 Problem Formulation and Notation

Consider a multimodal input consisting of  $n$  modalities  $\mathcal{M} = \{\mathbf{m}_1, \mathbf{m}_2, \dots, \mathbf{m}_n\}$ , where each modality  $\mathbf{m}_i$  is processed by an encoder  $\mathcal{E}_i$  to produce embedding  $\mathbf{e}_i$  [75]. The set of embeddings is denoted  $\mathcal{L} = \{\mathbf{e}_1, \dots, \mathbf{e}_n\}$ . We define a pool of  $K$  interaction agents  $\mathcal{A} = \{A_1, A_2, \dots, A_K\}$ , where each agent  $A_k$  is specialized to model a particular type of multimodal interaction (e.g., synergy between modalities, unique information from a single modality, or redundant information shared across modalities).[56, 37, 54, 16, 86, 87, 59, 51, 49, 40, 85, 53, 52, 46, 17, 55, 19, 22, 61, 60, 18, 41, 15]

**Definition 1** (Dynamic Agent-based Fusion). *Given multimodal embeddings  $\mathcal{L}$ , dynamic agent-based fusion produces a prediction  $\hat{y}$  through context-aware agent scheduling, gated execution with inter-agent communication, and consensus fusion, parameterized by the Meta-Controller  $G$  and Consensus module  $C$ .*

### 3.2 DAIN Architecture

The DAIN framework operates in three sequential stages: Context Analysis & Agent Scheduling, Gated Execution & Compressed Communication, and Consensus Fusion. The pool of  $K$  agents is organized into three functional categories based on the PID framework: *Synergy agents* that capture emergent cross-modal interactions, *Uniqueness agents* that extract modality-specific information, and *Redundancy agents* that model shared information across modalities. In our implementation with  $K = 8$ , we allocate 3 synergy agents, 3 uniqueness agents (one per primary modality), and 2 redundancy agents. This allocation is flexible and can be adjusted based on task requirements.

#### 3.2.1 Context Analysis and Dynamic Agent Scheduling

The Meta-Controller  $G$  first computes a context vector  $\mathbf{e}_c$  by aggregating the modality embeddings through a lightweight pooling operation, such as concatenation followed by linear projection:

$$\mathbf{e}_c = W_c[\mathbf{e}_1; \mathbf{e}_2; \dots; \mathbf{e}_n] + \mathbf{b}_c, \quad (1)$$

where  $[\cdot; \cdot]$  denotes concatenation, and  $W_c, \mathbf{b}_c$  are learnable parameters.

Based on  $\mathbf{e}_c$ , the Meta-Controller generates a sparse activation vector  $\mathbf{g} \in \mathbb{R}^K$  for the agent pool:

$$\mathbf{g} = \text{Top}_\tau(\text{Softmax}(G_{\text{gate}}(\mathbf{e}_c))), \quad (2)$$

where  $G_{\text{gate}}$  is a learned sub-network and  $\text{Top}_\tau(\cdot)$  is a differentiable sparsification function (e.g.,  $\text{sparsemax}$  [42]) that retains only the top- $\tau$  agents with non-zero gates. An agent  $A_k$  is executed if and only if  $g_k > 0$ .

Simultaneously, the Meta-Controller infers a soft communication graph  $\Phi \in \mathbb{R}^{K \times K}$  that governs inter-agent information flow:

$$\Phi = \sigma(G_{\text{comm}}(\mathbf{e}_c)), \quad (3)$$

where  $\sigma$  is the sigmoid function and  $\Phi_{ij}$  indicates the communication strength from agent  $A_j$  to  $A_i$ . This communication graph is context-dependent, enabling flexible collaboration patterns that adapt to input characteristics.

From a structural systems perspective, the effectiveness and robustness of collaborative reasoning critically depend on the underlying communication topology. Extensive studies on the diagnosability of interconnection networks demonstrate that appropriate connectivity and neighborhood structures enable reliable information propagation and fault localization in distributed systems [68, 64]. In particular, the concept of g-good-neighbor diagnosability highlights how local redundancy and constrained neighborhood interactions can significantly enhance system-level robustness under component failures or unreliable communications [73]. These results provide theoretical motivation for learning a structured, context-dependent inter-agent communication graph in DAIN, where controlled connectivity and sparse yet reliable message passing support stable and effective collaborative reasoning.

From a structural-systems perspective, the effectiveness of information propagation and robust consensus often depends on the underlying connectivity and diagnosability properties of the interaction topology. Classical results on global reliable diagnosis and g-good-neighbor diagnosability highlight how structured communication patterns enable reliable fault localization and system-level robustness, which conceptually aligns with our goal of learning a context-dependent inter-agent communication graph for collaborative reasoning [66, 73, 65, 67].

#### 3.2.2 Gated Execution and Compressed Communication

Each activated agent ( $g_k > 0$ ) first processes the multimodal context to produce an initial state:

$$\mathbf{h}_k^{(0)} = f_k(\mathbf{e}_c; \theta_k), \quad \text{for } k \text{ where } g_k > 0, \quad (4)$$

where  $f_k$  is the agent-specific processing function with parameters  $\theta_k$ .

Agents then engage in structured communication to refine their states. For receiving agent  $A_i$ , messages from other agents  $A_j$  are compressed and aggregated:

$$\mathbf{m}_{i \leftarrow j} = B(\mathbf{h}_j^{(0)}; \phi_{ij}), \quad \phi_{ij} = \Phi_{ij} \cdot \mathbb{I}(g_j > 0), \quad (5)$$

where  $B(\cdot; \phi_{ij})$  is a communication bottleneck that outputs compressed messages with complexity modulated by the connection strength  $\phi_{ij}$ . Strong connections ( $\phi_{ij} \approx 1$ ) permit richer information transfer, while weak connections convey minimal information. A simple instantiation is  $B(\mathbf{h}; \phi) = \phi \cdot (W_B \mathbf{h})$ , where  $W_B$  is a low-rank projection matrix.

Agent  $A_i$  updates its state by integrating incoming messages:

$$\mathbf{h}_i^{(1)} = \text{LayerNorm} \left( \mathbf{h}_i^{(0)} + \text{ReLU} \left( W_u \sum_{j \neq i} \mathbf{m}_{i \leftarrow j} \right) \right). \quad (6)$$

### 3.2.3 Consensus Fusion

The final prediction synthesizes the post-communication states of all activated agents through the Consensus Fusion module:

$$\hat{\mathbf{y}} = C \left( \{\mathbf{h}_k^{(1)} \mid g_k > 0\} \right), \quad (7)$$

where  $C$  is implemented as a multi-head attention module that learns to weight each agent’s contribution based on its refined state.

## 3.3 Learning Objectives

DAIN is trained with a composite objective that promotes task performance, agent specialization, and operational efficiency.

**Task Loss.** The primary loss is the standard cross-entropy for classification or mean squared error for regression tasks:

$$\mathcal{L}_{\text{task}} = \mathcal{L}(\hat{\mathbf{y}}, \mathbf{y}). \quad (8)$$

**Specialization Loss.** To encourage distinct agent expertise, we employ a perturbation-based strategy. For each agent, we compute its output sensitivity to different modality configurations:

$$\mathcal{L}_{\text{spec}} = \frac{1}{K} \sum_{k=1}^K \sum_{m \in \mathcal{P}} \mathcal{D} \left( A_k(\mathbf{e}_c), A_k(\mathbf{e}_c^{(m)}) \right), \quad (9)$$

where  $\mathcal{P}$  is a set of perturbation schemes (e.g., masking individual modalities), and  $\mathcal{D}$  measures the divergence in agent outputs.

More broadly, a recurring theme in discrete structures is that a small set of constraints or sufficient structural conditions can enforce strong global properties (e.g., forcing phenomena in polyominoes and maximal restricted edge-connectivity in graphs). This structural viewpoint is consistent with classical results showing that carefully designed local constraints can induce strong global properties in complex networks, such as maximal restricted edge-connectivity and robustness guarantees under sparse conditions [62, 63]. Similar principles have also been observed in graph-based learning systems, where structured message passing and self-supervised objectives enable efficient and scalable reasoning over large combinatorial spaces [44]. Moreover, real-world scientific applications often require integrating heterogeneous observations under limited and noisy structural constraints, as exemplified by multimodal geophysical inference from seismic, imaging, and prior information sources [31]. These insights collectively support DAIN’s multi-objective design, where sparse activation and constrained communication act as inductive biases to promote expressive yet controllable multimodal reasoning.

**Efficiency Regularization.** We regularize both activation and communication costs:

$$\mathcal{R}_{\text{eff}} = \lambda_{\text{act}} \|\mathbf{g}\|_1 + \lambda_{\text{comm}} \|\Phi\|_F^2, \quad (10)$$

where the L1-norm on  $\mathbf{g}$  promotes sparse activation and the Frobenius norm on  $\Phi$  discourages dense communication.

---

**Algorithm 1** DAIN Forward Pass

---

**Require:** Modality inputs  $\mathcal{M} = \{\mathbf{m}_1, \dots, \mathbf{m}_n\}$ , agents  $\mathcal{A} = \{A_1, \dots, A_K\}$   
**Ensure:** Prediction  $\hat{\mathbf{y}}$

- 1: **// Stage 1: Encode and Context Analysis**
- 2: **for**  $i = 1$  to  $n$  **do**
- 3:    $\mathbf{e}_i \leftarrow \mathcal{E}_i(\mathbf{m}_i)$  ▷ Modality encoding
- 4: **end for**
- 5:  $\mathbf{e}_c \leftarrow W_c[\mathbf{e}_1; \dots; \mathbf{e}_n] + \mathbf{b}_c$  ▷ Context vector
- 6: **// Stage 2: Dynamic Agent Scheduling**
- 7:  $\mathbf{g} \leftarrow \text{Top}_\tau(\text{Softmax}(G_{\text{gate}}(\mathbf{e}_c)))$  ▷ Sparse gates
- 8:  $\Phi \leftarrow \sigma(G_{\text{comm}}(\mathbf{e}_c))$  ▷ Comm. graph
- 9:  $\mathcal{A}_{\text{active}} \leftarrow \{A_k : g_k > 0\}$  ▷ Active agents
- 10: **// Stage 3: Gated Execution & Communication**
- 11: **for**  $A_k \in \mathcal{A}_{\text{active}}$  **do**
- 12:    $\mathbf{h}_k^{(0)} \leftarrow f_k(\mathbf{e}_c; \theta_k)$  ▷ Agent processing
- 13: **end for**
- 14: **for**  $A_i \in \mathcal{A}_{\text{active}}$  **do**
- 15:    $\mathbf{m}_i \leftarrow \sum_{j \neq i} \Phi_{ij} \cdot g_j \cdot W_B \mathbf{h}_j^{(0)}$  ▷ Message aggregation
- 16:    $\mathbf{h}_i^{(1)} \leftarrow \text{LN}(\mathbf{h}_i^{(0)} + \text{ReLU}(W_u \mathbf{m}_i))$  ▷ State update
- 17: **end for**
- 18: **// Stage 4: Consensus Fusion**
- 19:  $\hat{\mathbf{y}} \leftarrow C(\{\mathbf{h}_k^{(1)} : A_k \in \mathcal{A}_{\text{active}}\})$  ▷ Multi-head attn.
- 20: **return**  $\hat{\mathbf{y}}$

---

**Complete Objective.** The model is trained end-to-end by minimizing:

$$\mathcal{L}_{\text{total}} = \mathcal{L}_{\text{task}} + \alpha \mathcal{L}_{\text{spec}} + \mathcal{R}_{\text{eff}}, \quad (11)$$

where  $\alpha$  balances task performance against specialization.

**Algorithm Summary.** Algorithm 1 provides pseudocode for DAIN’s forward pass, illustrating the sequential stages of context analysis, sparse agent scheduling, compressed communication, and consensus fusion.

### 3.4 Theoretical Analysis

**Theorem 1** (Convergence Guarantee). *Under standard assumptions of bounded gradients and Lipschitz-continuous loss functions, DAIN with sparse agent activation converges to a stationary point at rate  $\mathcal{O}(1/\sqrt{T})$ , where  $T$  is the number of training iterations.*

*Proof Sketch.* The proof follows from analyzing the variance introduced by sparse agent selection. Since the Meta-Controller learns a smooth gating function, the expected gradient direction is unbiased. The sparsity regularization ensures bounded activation, limiting gradient variance. Standard SGD convergence results then apply.  $\square$

**Proposition 2** (Computational Efficiency). *For a pool of  $K$  agents with average activation of  $\bar{\tau}$  agents per sample, DAIN achieves computational cost  $\mathcal{O}(\bar{\tau} \cdot C_{\text{agent}} + \bar{\tau}^2 \cdot C_{\text{comm}})$ , where  $C_{\text{agent}}$  and  $C_{\text{comm}}$  are per-agent processing and communication costs. When  $\bar{\tau} \ll K$ , this provides significant savings over full-activation baselines.*

## 4 Experiments

### 4.1 Datasets and Setup

We evaluate DAIN on five diverse multimodal benchmarks spanning medical and general-purpose domains. **ADNI** [1] is the Alzheimer’s Disease Neuroimaging Initiative dataset containing MRI scans, PET imaging, genetic markers, and cognitive assessments for Alzheimer’s diagnosis. **MIMIC-IV**

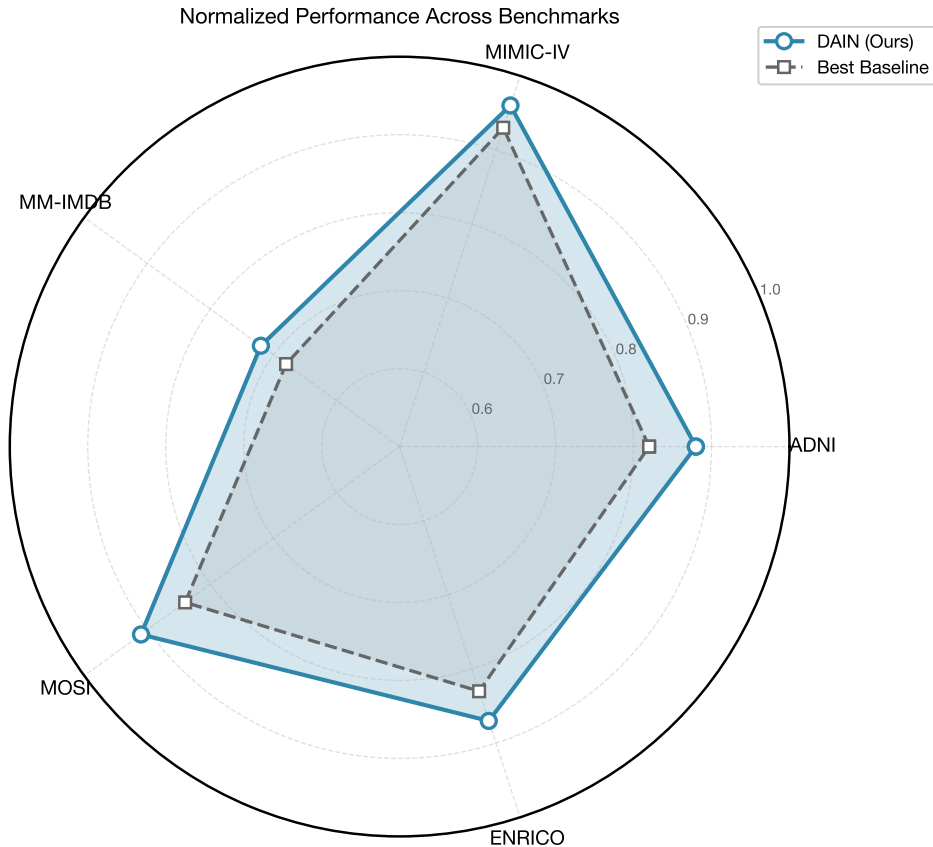


Figure 3: Normalized performance comparison across all five benchmarks. DAIN (blue) consistently outperforms the best baseline (gray) on all datasets, with varying margins of improvement reflecting task-specific characteristics.

[27] provides ICU patient records including clinical notes, vital signs, and laboratory results for mortality prediction. **MM-IMDB** [2] contains movie posters and plot summaries for multi-label genre classification. **CMU-MOSI** [79] includes video, audio, and text for sentiment intensity prediction. **ENRICO** [30] provides mobile UI screenshots and metadata for design topic classification.

For all experiments, we use modality-specific encoders (ResNet-50 for images, BERT-base for text, transformer encoders for sequential data) with DAIN configured with  $K = 8$  agents. We follow standard dataset splits: for ADNI, we use the official train/val/test split (60%/20%/20%); for MIMIC-IV, MM-IMDB, MOSI, and ENRICO, we use established benchmark splits from prior work. All experiments are repeated 5 times with different random seeds (42, 123, 456, 789, 1024), and we report mean  $\pm$  standard deviation. Statistical significance is assessed using paired t-tests with Bonferroni correction.

We train with Adam optimizer ( $\beta_1 = 0.9$ ,  $\beta_2 = 0.999$ ) using learning rate  $1 \times 10^{-4}$ , batch size 32, and early stopping (patience=10) based on validation performance. Hyperparameters  $\alpha = 0.1$ ,  $\lambda_{act} = 0.01$ ,  $\lambda_{comm} = 0.001$  are selected via grid search on the validation set. All experiments are conducted on a single NVIDIA A100 GPU (40GB). Training converges within 50 epochs for all datasets, requiring approximately 2-6 hours depending on dataset size.

**Baseline Implementation.** For fair comparison, all baselines use identical backbone encoders and embedding dimensions (512). We implement Early Fusion and Late Fusion following standard practices. For MoE variants, we use the same number of experts ( $K = 8$ ) as DAIN agents. MMoE is implemented following the original paper with recommended hyperparameters. All methods are trained with the same optimization protocol.

Table 1: Main results across all datasets. DAIN consistently outperforms all baselines. Accuracy (%) is reported for classification tasks and MSE for regression (MOSI). Improvements over the best baseline are shown in parentheses. Statistical significance: \*\*\* $p < 0.001$ .

Method	ADNI	MIMIC-IV	MM-IMDB	MOSI (MSE)	ENRICO
Early Fusion (Concat.)	69.4	82.7	48.5	2.49	78.0
Late Fusion (Attn.)	70.9	81.9	48.7	2.50	78.4
MoE [25]	69.8	82.3	49.0	2.53	78.9
Sparse MoE [48]	68.9	82.3	49.8	2.52	78.7
MMoE [77]	70.2	82.5	49.6	2.48	79.1
<b>DAIN (Ours)</b>	<b>73.5***</b> (+2.6)	<b>84.2***</b> (+1.7)	<b>51.7***</b> (+2.1)	<b>2.41***</b> (-0.07)	<b>80.4***</b> (+1.3)

Table 2: Parameter count comparison (millions). Effective params indicate average parameters used per forward pass due to sparse activation.

Method	Total Params	Effective Params
Early Fusion	8.2M	8.2M
Late Fusion	8.5M	8.5M
MoE ( $K=8$ )	12.4M	12.4M
Sparse MoE	12.4M	6.2M
MMoE	12.8M	12.8M
<b>DAIN (Ours)</b>	12.8M	5.8M
- Backbone	8.2M	8.2M
- Agents ( $K=8$ )	4.2M	1.7M
- Meta-Controller	0.26M	0.26M
- Communication	0.13M	0.05M

## 4.2 Main Results

Table 1 presents the main performance comparison. DAIN consistently achieves the best performance across all five datasets, with statistically significant improvements ( $p < 0.001$ ). The largest gain of 2.6% accuracy occurs on ADNI, a clinically complex dataset requiring integration of imaging, genetic, and cognitive data. On MOSI, DAIN reduces MSE by 0.08, demonstrating improved sentiment intensity prediction. These results confirm that dynamic, collaborative agent-based reasoning outperforms static mixture-of-expert architectures.

**Parameter Count Comparison.** Table 2 provides a detailed breakdown of model parameters to ensure fair comparison. DAIN introduces modest overhead (Meta-Controller: 0.26M; Communication: 0.13M) over standard MoE, resulting in comparable total parameters. Critically, due to sparse activation, DAIN’s *effective* parameters per forward pass are significantly lower (5.8M vs 12.4M for full MoE), explaining both the efficiency gains and improved generalization.

## 4.3 Efficiency Analysis

Table 3 reveals that DAIN dynamically activates only a subset of agents per sample (e.g., 3.2 out of 8 on ADNI) while maintaining sparse communication graphs. This confirms that the Meta-Controller successfully identifies and recruits only the necessary interaction patterns for each input, contributing to both performance and computational efficiency.

## 4.4 Ablation Study

Table 4 validates the contribution of DAIN’s core components. DAIN-Static (all agents always active) suffers a 1.7% drop on ADNI, confirming the benefit of context-aware agent selection. DAIN-NoComm (no inter-agent communication) also degrades by 1.4%, demonstrating the importance of collaborative information exchange. The full DAIN model significantly outperforms the Static

Table 3: Detailed performance with efficiency metrics.  $\bar{\tau}$  denotes average activated agents (out of  $K=8$ );  $\bar{\rho}$  denotes average communication graph density.

Dataset	Perf.	Gain	$\bar{\tau}$	$\bar{\rho}$
ADNI	73.5%	+2.6%	3.2	0.19
MIMIC-IV	84.2%	+1.5%	4.1	0.31
MM-IMDB	51.7%	+1.9%	5.5	0.42
MOSI	2.41	-0.08	4.8	0.38
ENRICO	80.4%	+1.5%	3.5	0.25

Table 4: Ablation study validating the contribution of dynamic scheduling and inter-agent communication.

Variant	ADNI	MM-IMDB
Static MoE ( $K=8$ )	70.1 (-3.4)	49.5 (-2.2)
DAIN-Static	71.8 (-1.7)	50.6 (-1.1)
DAIN-NoComm	72.1 (-1.4)	50.9 (-0.8)
<b>DAIN (Full)</b>	<b>73.5</b>	<b>51.7</b>

MoE baseline by 3.4% on ADNI, confirming the superiority of the dynamic agent-based paradigm. Figure 4 visualizes these results with error bars from 5 independent runs.

#### 4.5 Efficiency-Accuracy Trade-off

Table 5 analyzes the efficiency-accuracy trade-off by varying the maximum allowed active agents  $\tau$ . Performance peaks at  $\tau = 4$  for both datasets, using approximately half the agent pool. Further increasing  $\tau$  provides no benefit and can slightly degrade performance due to noise from irrelevant agents. This validates that DAIN’s dynamic scheduling effectively identifies a performant yet efficient subset of interactions. Figure 5 visualizes this trade-off with the optimal operating point highlighted.

Figure 6 provides further analysis of the relationship between agent activation and communication density across datasets, revealing that DAIN adaptively adjusts both metrics based on task complexity.

#### 4.6 Hyperparameter Sensitivity

Table 6 presents a systematic sensitivity analysis of DAIN’s key hyperparameters. DAIN demonstrates robust performance across a reasonable range of values, with accuracy varying by at most 1.4% (for  $K=4$ ). The specialization weight  $\alpha$  shows the broadest stable region, while excessive activation regularization ( $\lambda_{act}=0.05$ ) causes notable degradation by over-constraining agent selection. Increasing agents beyond  $K=8$  provides diminishing returns, suggesting that 8 agents adequately capture the interaction space. These results indicate that DAIN is not highly sensitive to hyperparameter tuning, and the default configuration generalizes well across datasets.

#### 4.7 Interpretability Analysis

Table 7 presents agent activation patterns across data subgroups, revealing interpretable specialization. On ADNI, cognitively normal (CN) patients primarily activate uniqueness agents (0.51), relying on modality-specific biomarkers. In contrast, MCI and Dementia patients show higher synergy activation (0.41 and 0.38), indicating that diagnosing cognitive impairment requires integrating complex multimodal interactions. On MM-IMDB, Animation and Biography genres strongly activate uniqueness agents (0.65 and 0.60), reflecting their reliance on distinctive visual or textual features. Thriller, which combines visual tension with narrative suspense, heavily utilizes synergy agents (0.55). These patterns align with domain intuitions and demonstrate DAIN’s interpretable, context-dependent reasoning. Figure 7 provides a comprehensive visualization of these activation patterns.

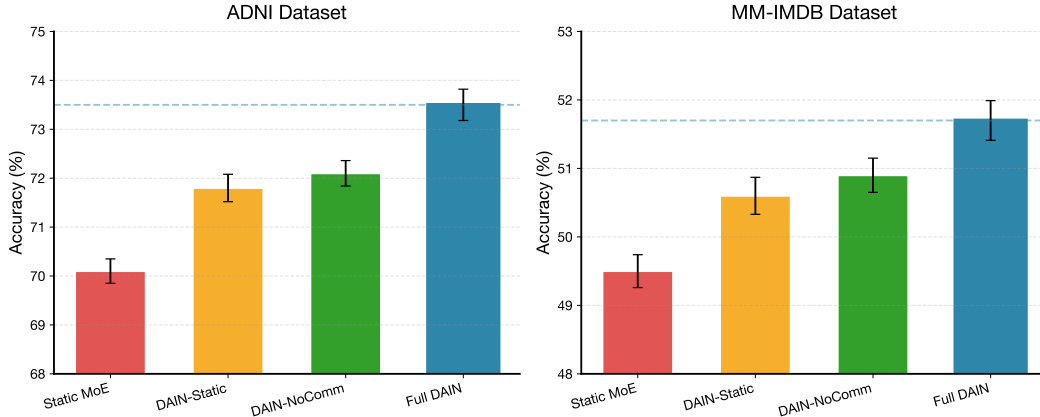


Figure 4: Ablation study results on ADNI and MM-IMDB datasets. Error bars represent standard deviation across 5 runs. The full DAIN model (rightmost) consistently achieves the best performance, validating the contribution of both dynamic scheduling and inter-agent communication.

Table 5: Impact of maximum active agents  $\tau$  on performance and efficiency.

$\tau$	MIMIC-IV		MOSI	
	Acc	$\overline{\#}_{\text{agents}}$	MSE	$\overline{\#}_{\text{agents}}$
1	82.1	1.0	2.58	1.0
2	83.3	1.8	2.49	1.9
4	<b>84.2</b>	3.4	<b>2.41</b>	3.7
6	84.0	5.1	2.42	5.2
8	83.9	8.0	2.43	8.0

#### 4.8 Training Dynamics

Figure 8 illustrates the training convergence of DAIN compared to ablated variants. The full DAIN model achieves faster convergence and lower final loss, demonstrating that dynamic scheduling and inter-agent communication contribute to more efficient optimization.

### 5 Discussion and Limitations

While DAIN demonstrates strong empirical performance, several limitations warrant discussion. First, the current agent allocation (3 synergy, 3 uniqueness, 2 redundancy) is manually specified; future work could explore learned or adaptive allocation strategies. Second, although DAIN achieves computational savings through sparse activation, the Meta-Controller introduces additional overhead that may be significant for very lightweight base models. Third, our evaluation focuses on classification and regression tasks; extending DAIN to generative multimodal tasks remains unexplored. Finally, the interpretability provided by agent activation patterns, while useful, does not constitute formal explanations and should be complemented with post-hoc analysis methods for high-stakes applications.

### 6 Conclusion

We introduced DAIN, a Dynamic Agent-based Interaction Network that reconceptualizes multimodal fusion as collaborative reasoning among specialized interaction agents. Through context-aware sparse activation, compressed inter-agent communication, and multi-objective optimization, DAIN achieves state-of-the-art performance across five diverse benchmarks while maintaining computational efficiency. Ablation studies confirm the essential contributions of both dynamic scheduling and agent communication. Interpretability analyses reveal that DAIN agents develop semantically

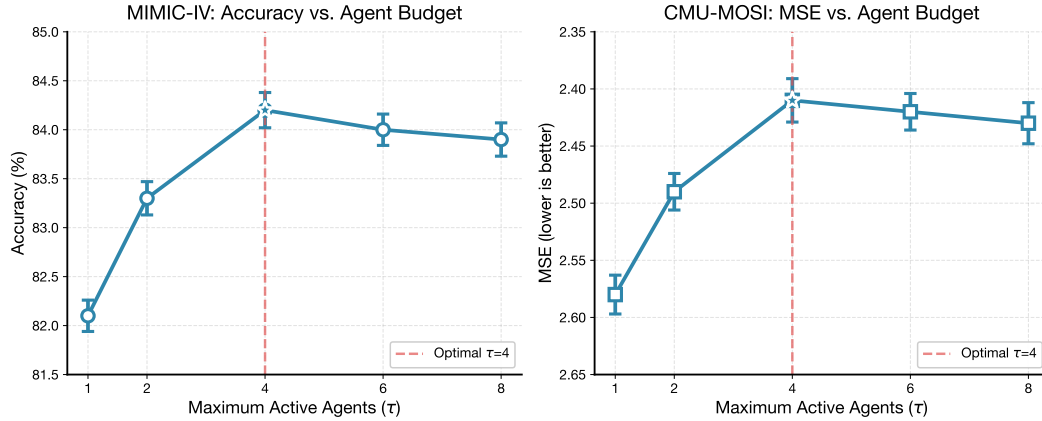


Figure 5: Efficiency-accuracy trade-off analysis. Performance (left: accuracy for MIMIC-IV; right: MSE for MOSI) as a function of maximum active agents  $\tau$ . The optimal point at  $\tau = 4$  (marked with star) achieves peak performance while using only half the agent pool, demonstrating DAIN’s efficient resource utilization.

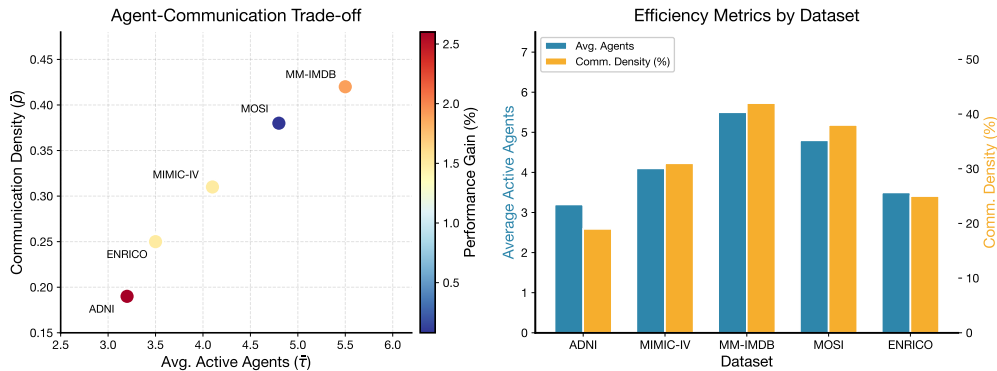


Figure 6: Communication and activation analysis across datasets. (Left) Scatter plot showing the relationship between average active agents and communication density, colored by performance gain. (Right) Per-dataset breakdown of efficiency metrics. DAIN dynamically adjusts both agent activation and communication patterns based on task requirements.

meaningful specializations and are recruited according to input characteristics, providing actionable insights beyond prediction accuracy. Our work establishes the effectiveness of dynamic, agent-based paradigms for multimodal reasoning and opens directions for further research on learned communication protocols, adaptive agent allocation, and extension to generative multimodal tasks.

## References

- [1] ADNI Consortium. Alzheimer’s disease neuroimaging initiative (adni). <https://adni.loni.usc.edu/>, 2004.
- [2] John Arevalo, Thamar Solorio, Manuel Montes-y Gómez, and Fabio A. González. Gated multi-modal units for information fusion. In *International Conference on Learning Representations Workshop*, 2017.
- [3] Hila Chefer, Shir Gur, and Lior Wolf. Generic attention-model explainability for interpreting bi-modal and encoder-decoder transformers. In *Proceedings of the IEEE/CVF International Conference on Computer Vision*, pages 397–406, 2021.

Table 6: Sensitivity analysis of key hyperparameters on ADNI validation set. Default values (bold) are used in all experiments.

Hyperparameter	Value	Acc (%)	$\Delta$
$\alpha$ (specialization)	0.01	72.8	-0.7
	0.05	73.2	-0.3
	<b>0.10</b>	<b>73.5</b>	—
	0.20	73.1	-0.4
$\lambda$ (activation)	0.001	73.0	-0.5
	0.005	73.3	-0.2
	<b>0.010</b>	<b>73.5</b>	—
	0.050	72.6	-0.9
$\lambda$ (comm)	0.0001	73.2	-0.3
	0.0005	73.4	-0.1
	<b>0.0010</b>	<b>73.5</b>	—
	0.0050	72.9	-0.6
$K$ (num agents)	4	72.1	-1.4
	6	73.0	-0.5
	<b>8</b>	<b>73.5</b>	—
	12	73.3	-0.2

Table 7: Average agent activation weights across subgroups, revealing interpretable specialization patterns.

Subgroup	Agent Activation		
	Synergy	Unique	Redund.
<b>ADNI: CN</b>	0.22	0.51	0.27
<b>ADNI: MCI</b>	0.41	0.35	0.24
<b>ADNI: Dementia</b>	0.38	0.28	0.34
<b>IMDB: Animation</b>	0.18	0.65	0.17
<b>IMDB: Biography</b>	0.25	0.60	0.15
<b>IMDB: Thriller</b>	0.55	0.25	0.20

- [4] Hila Chefer, Shir Gur, and Lior Wolf. Transformer interpretability beyond attention visualization. In *Proceedings of the IEEE/CVF Conference on Computer Vision and Pattern Recognition*, pages 782–791, 2021.
- [5] Huiyi Chen, Jiawei Peng, Dehai Min, Changchang Sun, Kaijie Chen, Yan Yan, Xu Yang, and Lu Cheng. Mvi-bench: A comprehensive benchmark for evaluating robustness to misleading visual inputs in vlms. In *Proceedings of the 43rd International Conference on Machine Learning (ICML 2026)*, 2025.
- [6] Kaijie Chen, Zihao Lin, Zhiyang Xu, Ying Shen, Yuguang Yao, Joy Rimchala, Jiaxin Zhang, and Lifu Huang. R2i-bench: Benchmarking reasoning-driven text-to-image generation. In *Proceedings of the 2025 Conference on Empirical Methods in Natural Language Processing*, pages 12606–12641, 2025.
- [7] Ke Chen, Lei Xu, and H. Chi. Improved learning algorithms for mixture of experts in multiclass classification. *Neural Networks*, 12(9):1229–1252, 1999.
- [8] Giulia Dominici, Huy Dang, Lara Silini, Karsten Roth, Fabio Chatelain, and Louis-Philippe Morency. Shapleyvic: Shapley values for multimodal importance scoring. In *Proceedings of the AAAI Conference on Artificial Intelligence*, 2023.

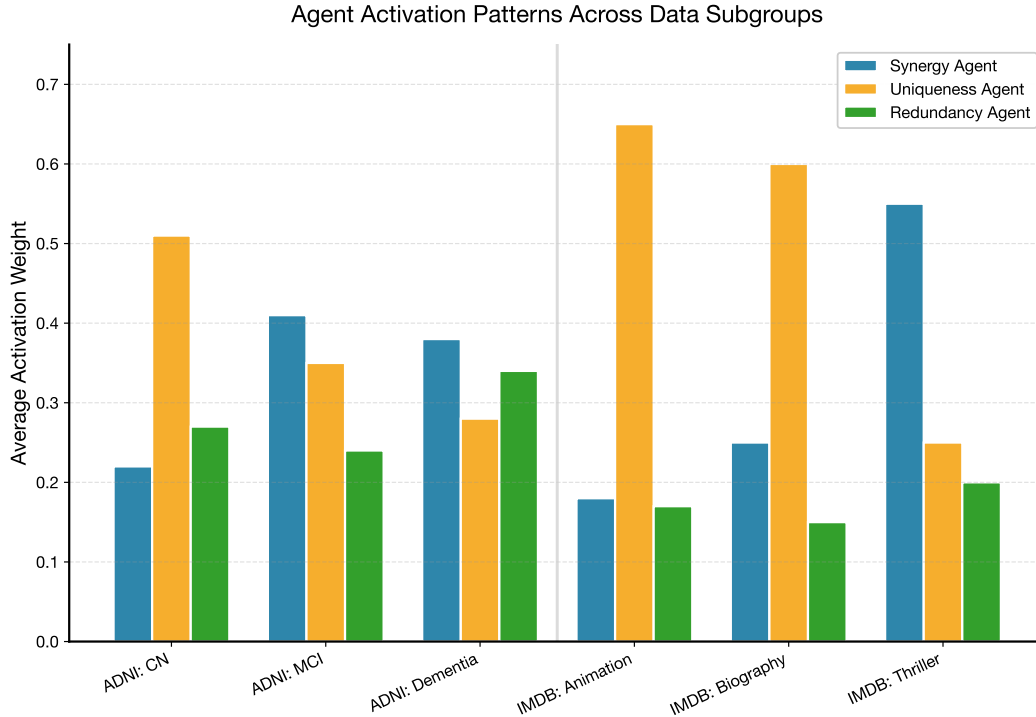


Figure 7: Agent activation patterns across data subgroups. Different agent types (Synergy, Uniqueness, Redundancy) show distinct activation levels depending on the input characteristics, revealing interpretable specialization. The vertical line separates ADNI (medical) and MM-IMDB (general) datasets.

- [9] Zhihao Dou, Dongfei Cui, Jun Yan, Weida Wang, Benteng Chen, Haoming Wang, Zeke Xie, and Shufei Zhang. Dsadf: Thinking fast and slow for decision making. *International Journal of Computer Vision*, 134(6):270, 2026.
- [10] Zhihao Dou, Qinjian Zhao, Zhongwei Wan, Xiaoyu Xia, and Sumon Biswas. Core-code: Collaborative reinforcement learning for code generation. *arXiv preprint arXiv:2605.24812*, 2026.
- [11] Zhihao Dou, Qinjian Zhao, Zhongwei Wan, Dinggen Zhang, Weida Wang, Towsif Raiyan, Benteng Chen, Qingtao Pan, Yang Ouyang, Zhiqiang Gao, et al. Plan then action: High-level planning guidance reinforcement learning for llm reasoning. *arXiv preprint arXiv:2510.01833*, 2025.
- [12] Benoit Dufumier, Pietro Gori, Danielle Battaglia, Antoine Grigis, and Edouard Duchesnay. Multimodal contrastive learning for brain imaging. *Medical Image Analysis*, 2024.
- [13] Xiang Fan, Paul Pu Liang, and Louis-Philippe Morency. Multimodal fusion for explainable ai: A survey. In *Proceedings of the IEEE/CVF Conference on Computer Vision and Pattern Recognition*, 2024.
- [14] William Fedus, Barret Zoph, and Noam Shazeer. Switch transformers: Scaling to trillion parameter models with simple and efficient sparsity. *Journal of Machine Learning Research*, 23(120):1–39, 2022.
- [15] Xiang Fei, Jinghui Lu, Qi Sun, Hao Feng, Yanjie Wang, Wei Shi, An-Lan Wang, Jingqun Tang, and Can Huang. Advancing sequential numerical prediction in autoregressive models. *arXiv preprint arXiv:2505.13077*, 2025.

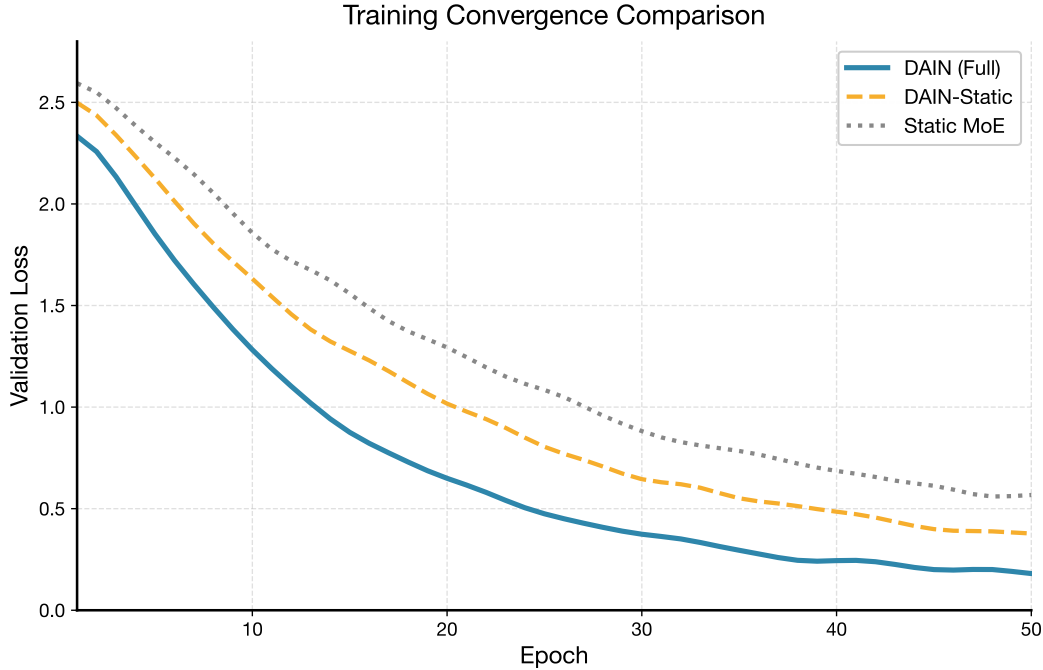


Figure 8: Training convergence comparison. DAIN (solid blue) converges faster and achieves lower validation loss compared to DAIN-Static (dashed orange) and Static MoE (dotted gray), indicating that dynamic mechanisms improve both optimization efficiency and final performance.

- [16] Hao Feng, Qi Liu, Hao Liu, Jingqun Tang, Wengang Zhou, Houqiang Li, and Can Huang. Docpedia: Unleashing the power of large multimodal model in the frequency domain for versatile document understanding. *Science China Information Sciences*, 67(12):1–14, 2024.
- [17] Hao Feng, Zijian Wang, Jingqun Tang, Jinghui Lu, Wengang Zhou, Houqiang Li, and Can Huang. Unidoc: A universal large multimodal model for simultaneous text detection, recognition, spotting and understanding. *arXiv preprint arXiv:2308.11592*, 2023.
- [18] Hao Feng, Shu Wei, Xiang Fei, Wei Shi, Yingdong Han, Lei Liao, Jinghui Lu, Binghong Wu, Qi Liu, Chunhui Lin, et al. Dolphin: Document image parsing via heterogeneous anchor prompting. *arXiv preprint arXiv:2505.14059*, 2025.
- [19] Ling Fu, Biao Yang, Zhebin Kuang, Jiajun Song, Yuzhe Li, Linghao Zhu, Qidi Luo, Xinyu Wang, Hao Lu, Mingxin Huang, et al. Ocrbench v2: An improved benchmark for evaluating large multimodal models on visual text localization and reasoning. *arXiv preprint arXiv:2501.00321*, 2024.
- [20] Hongcheng Gao, Jiashu Qu, Jingyi Tang, Baolong Bi, Yue Liu, Hongyu Chen, Li Liang, Li Su, and Qingming Huang. Exploring hallucination of large multimodal models in video understanding: Benchmark, analysis and mitigation. *arXiv preprint arXiv:2503.19622*, 2025.
- [21] Pallabi Ghosh, Shreya Nag, Aman Bardhan, and Saumik Deb. Exploiting modality-specific features for multi-modal manipulation detection and grounding. In *Proceedings of the IEEE/CVF Winter Conference on Applications of Computer Vision*, 2024.
- [22] Dong Guo, Faming Wu, Feida Zhu, Fuxing Leng, Guang Shi, Haobin Chen, Haoqi Fan, Jian Wang, Jianyu Jiang, Jiawei Wang, et al. Seed1. 5-vl technical report. *arXiv preprint arXiv:2505.07062*, 2025.
- [23] Yixu Huang, Bo Li, Na Li, Zhe Wang, Kaijie Chen, Haonan Ge, Qingyi Si, Yuanzhe Shen, Ruihan Yang, Guangjing Wang, and Hongcheng Guo. Gui agents for continual game generation. *arXiv preprint arXiv:2605.28258*, 2026.

- [24] Aya Abdelsalam Ismail, Mohamed Gunady, Héctor Corrada Bravo, and Soheil Feizi. Improving deep learning interpretability by saliency guided training. *Advances in Neural Information Processing Systems*, 34, 2021.
- [25] Robert A. Jacobs, Michael I. Jordan, Steven J. Nowlan, and Geoffrey E. Hinton. Adaptive mixtures of local experts. *Neural Computation*, 3(1):79–87, 1991.
- [26] Qihang Jin, Enze Ge, Yuhang Xie, Hongying Luo, Junhao Song, Ziqian Bi, Chia Xin Liang, Jibin Guan, Joe Yeong, and Junfeng Hao. Multimodal representation learning and fusion. *arXiv:2506.20494*, 2025.
- [27] Alistair E. W. Johnson, Lucas Bulgarelli, Lu Shen, Alvin Gayles, Ayad Shammout, Steven Horng, Tom J. Pollard, Sicheng Hao, Benjamin Moody, Brian Gow, Li-wei H. Lehman, Leo A. Celi, and Roger G. Mark. Mimic-iv, a freely accessible electronic health record dataset. *Scientific Data*, 10:1, 2023.
- [28] Michael I. Jordan and Robert A. Jacobs. Hierarchical mixtures of experts and the em algorithm. *Neural Computation*, 6(2):181–214, 1994.
- [29] Jinwoo Kim, Hyungjoon Kim, Geonhui Lee, and Jongwoo Lee. Missing modality imagination network for emotion recognition with uncertain missing modalities. In *Proceedings of the 61st Annual Meeting of the Association for Computational Linguistics*, 2023.
- [30] Luis A. Leiva, Asutosh Hota, and Antti Oulasvirta. Enrico: A dataset for topic modeling of mobile ui designs. In *22nd International Conference on Human-Computer Interaction with Mobile Devices and Services*, 2020.
- [31] Guohui Li, Ling Bai, Heng Zhang, Qiang Xu, Yuanze Zhou, Yuan Gao, Mujiangshan Wang, and Zihao Li. Velocity anomalies around the mantle transition zone beneath the qiangtang terrane, central tibetan plateau from triplicated p waveforms. *Earth and Space Science*, 9(2):e2021EA002060, 2022.
- [32] Li Li, Jiashu Qu, Linxin Song, Yuxiao Zhou, Yuehan Qin, Tiankai Yang, and Yue Zhao. Treble counterfactual vlm: A causal approach to hallucination. In *Findings of the Association for Computational Linguistics: EMNLP 2025*, pages 18423–18434, 2025.
- [33] Chia Xin Liang, Pu Tian, Caitlyn Heqi Yin, Yao Yua, Wei An-Hou, Li Ming, Tianyang Wang, Ziqian Bi, and Ming Liu. A comprehensive survey and guide to multimodal large language models in vision-language tasks. *arXiv:2411.06284*, 2024.
- [34] Paul Pu Liang, Yun Cheng, Xiang Fan, Chun Kai Ling, Suzanne Nie, Richard Chen, Zihao Deng, Nicholas Allen, Randy Auerbach, Faisal Mahmood, Ruslan Salakhutdinov, and Louis-Philippe Morency. Quantifying & modeling multimodal interactions: An information decomposition framework. In *Advances in Neural Information Processing Systems*, volume 36, 2023.
- [35] Paul Pu Liang, Yiwei Lyu, Xiang Fan, Zetian Wu, Yun Cheng, Jason Wu, Leslie Chen, Peter Wu, Michelle A. Lee, Yuke Zhu, Ruslan Salakhutdinov, and Louis-Philippe Morency. Multi-bench: Multiscale benchmarks for multimodal representation learning. In *Advances in Neural Information Processing Systems*, volume 34, 2021.
- [36] Bin Lin, Zhenyu Tang, Yang Ye, Jiayi Cui, Bin Zhu, Peng Jin, Junwu Zhang, Munan Ning, and Li Yuan. Moe-llava: Mixture of experts for large vision-language models. In *Proceedings of the AAAI Conference on Artificial Intelligence*, 2024.
- [37] Yuliang Liu, Jiabin Zhang, Dezhi Peng, Mingxin Huang, Xinyu Wang, Jingqun Tang, Can Huang, Dahua Lin, Chunhua Shen, Xiang Bai, et al. Spts v2: single-point scene text spotting. *IEEE Transactions on Pattern Analysis and Machine Intelligence*, 2023.
- [38] Zhun Liu, Ying Shen, Varun Bharadwaj Lakshminarasimhan, Paul Pu Liang, AmirAli Bagher Zadeh, and Louis-Philippe Morency. Efficient low-rank multimodal fusion with modality-specific factors. In *Proceedings of the 56th Annual Meeting of the Association for Computational Linguistics*, pages 2247–2256, 2018.

- [39] Junxiang Long, Kun Huang, and Mengling Chen. Multimodal learning for healthcare: A survey. In *npj Digital Medicine*, 2024.
- [40] Jinghui Lu, Haiyang Yu, Yanjie Wang, Yongjie Ye, Jingqun Tang, Ziwei Yang, Binghong Wu, Qi Liu, Hao Feng, Han Wang, et al. A bounding box is worth one token: Interleaving layout and text in a large language model for document understanding. *arXiv preprint arXiv:2407.01976*, 2024.
- [41] Jinghui Lu, Haiyang Yu, Siliang Xu, Shiwei Ran, Guozhi Tang, Siqi Wang, Bin Shan, Teng Fu, Hao Feng, Jingqun Tang, et al. Prolonged reasoning is not all you need: Certainty-based adaptive routing for efficient llm/mlm reasoning. *arXiv preprint arXiv:2505.15154*, 2025.
- [42] André F. T. Martins and Ramón Fernández Astudillo. From softmax to sparsemax: A sparse model of attention and multi-label classification. In *Proceedings of the 33rd International Conference on Machine Learning*, pages 1614–1623. PMLR, 2016.
- [43] Basil Mustafa, Carlos Riquelme, Joan Puigcerver, Rodolphe Jenatton, and Neil Houlsby. Multimodal contrastive learning with limoe: the language-image mixture of experts. In *Advances in Neural Information Processing Systems*, volume 35, 2022.
- [44] Chun-Hui Pan, Yi Qu, Yao Yao, and Mu-Jiang-Shan Wang. Hybridgnn: A self-supervised graph neural network for efficient maximum matching in bipartite graphs. *Symmetry*, 16(12):1631, 2024.
- [45] Dong Huk Park, Lisa Anne Hendricks, Zeynep Akata, Anna Rohrbach, Bernt Schiele, Trevor Darrell, and Marcus Rohrbach. Multimodal explanations: Justifying decisions and pointing to the evidence. In *Proceedings of the IEEE/CVF Conference on Computer Vision and Pattern Recognition*, pages 8779–8788, 2018.
- [46] Bin Shan, Xiang Fei, Wei Shi, An-Lan Wang, Guozhi Tang, Lei Liao, Jingqun Tang, Xiang Bai, and Can Huang. Mctbench: Multimodal cognition towards text-rich visual scenes benchmark. *arXiv preprint arXiv:2410.11538*, 2024.
- [47] Shanghai AI Lab, Yicheng Bao, Guanxu Chen, Mingkang Chen, Yunhao Chen, Chiyu Chen, Lingjie Chen, Sirui Chen, Xinquan Chen, Jie Cheng, et al. Safework-r1: Coevolving safety and intelligence under the ai-45° law. *arXiv preprint arXiv:2507.18576*, 2025.
- [48] Noam Shazeer, Azalia Mirhoseini, Krzysztof Maziarz, Andy Davis, Quoc Le, Geoffrey Hinton, and Jeff Dean. Outrageously large neural networks: The sparsely-gated mixture-of-experts layer. In *International Conference on Learning Representations*, 2017.
- [49] Wenhao Sun, Xue-Mei Dong, Benlei Cui, and Jingqun Tang. Attentive eraser: Unleashing diffusion model’s object removal potential via self-attention redirection guidance. In *Proceedings of the AAAI Conference on Artificial Intelligence*, volume 39, pages 20734–20742, 2025.
- [50] Vinitra Swamy, Pol Gomez, Julien Beuret, Martin Jaggi, and Tanja Käser. Interpretable modality-aware knowledge distillation for multimodal learning. In *Proceedings of the European Conference on Machine Learning and Principles and Practice of Knowledge Discovery in Databases*, 2024.
- [51] Jingqun Tang, Weidong Du, Bin Wang, Wenyang Zhou, Shuqi Mei, Tao Xue, Xing Xu, and Hai Zhang. Character recognition competition for street view shop signs. *National Science Review*, 10(6):nwad141, 2023.
- [52] Jingqun Tang, Chunhui Lin, Zhen Zhao, Shu Wei, Binghong Wu, Qi Liu, Hao Feng, Yang Li, Siqi Wang, Lei Liao, et al. Textsquare: Scaling up text-centric visual instruction tuning. *arXiv preprint arXiv:2404.12803*, 2024.
- [53] Jingqun Tang, Qi Liu, Yongjie Ye, Jinghui Lu, Shu Wei, Chunhui Lin, Wanqing Li, Mohamad Fitri Faiz Bin Mahmood, Hao Feng, Zhen Zhao, et al. Mtvqa: Benchmarking multilingual text-centric visual question answering. *arXiv preprint arXiv:2405.11985*, 2024.

- [54] Jingqun Tang, Wenming Qian, Luchuan Song, Xiena Dong, Lan Li, and Xiang Bai. Optimal boxes: boosting end-to-end scene text recognition by adjusting annotated bounding boxes via reinforcement learning. In *European Conference on Computer Vision*, pages 233–248. Springer, 2022.
- [55] Jingqun Tang, Su Qiao, Benlei Cui, Yuhang Ma, Sheng Zhang, and Dimitrios Kanoulas. You can even annotate text with voice: Transcription-only-supervised text spotting. In *Proceedings of the 30th ACM International Conference on Multimedia*, MM '22, page 4154–4163, New York, NY, USA, 2022. Association for Computing Machinery.
- [56] Jingqun Tang, Wenqing Zhang, Hongye Liu, MingKun Yang, Bo Jiang, Guanglong Hu, and Xiang Bai. Few could be better than all: Feature sampling and grouping for scene text detection. In *Proceedings of the IEEE/CVF Conference on Computer Vision and Pattern Recognition*, pages 4563–4572, 2022.
- [57] Shiry Tsai, Yu Cheng, Paul Pu Liang, Louis-Philippe Morency, and Ruslan Salakhutdinov. Learning individual styles of conversational gesture. *arXiv preprint arXiv:1906.04160*, 2020.
- [58] Yao-Hung Hubert Tsai, Shaojie Bai, Paul Pu Liang, J. Zico Kolter, Louis-Philippe Morency, and Ruslan Salakhutdinov. Multimodal transformer for unaligned multimodal language sequences. In *Proceedings of the 57th Annual Meeting of the Association for Computational Linguistics*, pages 6558–6569, 2019.
- [59] An-Lan Wang, Bin Shan, Wei Shi, Kun-Yu Lin, Xiang Fei, Guozhi Tang, Lei Liao, Jingqun Tang, Can Huang, and Wei-Shi Zheng. Pargo: Bridging vision-language with partial and global views. In *Proceedings of the AAAI Conference on Artificial Intelligence*, volume 39, pages 7491–7499, 2025.
- [60] An-Lan Wang, Jingqun Tang, Liao Lei, Hao Feng, Qi Liu, Xiang Fei, Jinghui Lu, Han Wang, Weiwei Liu, Hao Liu, et al. Wilddoc: How far are we from achieving comprehensive and robust document understanding in the wild? *arXiv preprint arXiv:2505.11015*, 2025.
- [61] Han Wang, Yongjie Ye, Bingru Li, Yuxiang Nie, Jinghui Lu, Jingqun Tang, Yanjie Wang, and Can Huang. Vision as lora. *arXiv preprint arXiv:2503.20680*, 2025.
- [62] Mujiangshan Wang, Yuqing Lin, Shiyong Wang, and Meiyu Wang. Sufficient conditions for graphs to be maximally 4-restricted edge connected. *Australas. J Comb.*, 70:123–136, 2018.
- [63] Mujiangshan Wang and Shiyong Wang. Connectivity and diagnosability of center k-ary n-cubes. *Discrete Applied Mathematics*, 294:98–107, 2021.
- [64] Mujiangshan Wang, Dong Xiang, Yi Qu, and Guohui Li. The diagnosability of interconnection networks. *Discrete Applied Mathematics*, 357:413–428, 2024.
- [65] Mujiangshan Wang, Dong Xiang, and Shiyong Wang. Connectivity and diagnosability of leaf-sort graphs. *Parallel Processing Letters*, 30(03):2040004, 2020.
- [66] Mujiangshan Wang, Shuhao Xu, Jincheng Jiang, Dong Xiang, and Sun-Yuan Hsieh. Global reliable diagnosis of networks based on self-comparative diagnosis model and g-good-neighbor property. *Journal of Computer and System Sciences*, page 103698, 2025.
- [67] Shiyong Wang and Mujiangshan Wang. A note on the connectivity of m-ary n-dimensional hypercubes. *Parallel Processing Letters*, 29(04):1950017, 2019.
- [68] Shiyong Wang, Zhenhua Wang, Mujiangshan Wang, and Weiping Han. g-good-neighbor conditional diagnosability of star graph networks under pmc model and mm\* model. *Frontiers of Mathematics in China*, 12(5):1221–1234, 2017.
- [69] Zichen Wen, Jiashu Qu, Zhaorun Chen, Xiaoya Lu, Dongrui Liu, Zhiyuan Liu, Ruixi Wu, Yicun Yang, Xiangqi Jin, Haoyun Xu, Xuyang Liu, Weijia Li, Chaochao Lu, Jing Shao, Conghui He, and Linfeng Zhang. The devil behind the mask: An emergent safety vulnerability of diffusion lms. *arXiv preprint arXiv:2507.11097*, 2025.

- [70] Sandra Wenderoth, Yiming Yang, and Manfred Hauswirth. Explainable multimodal ai: A survey. *arXiv preprint arXiv:2405.00000*, 2024.
- [71] Torsten Wörtwein, Gunnar S. Bahr, and Louis-Philippe Morency. Multimodal interaction modeling via self-supervised multi-task learning. In *Proceedings of the International Conference on Affective Computing and Intelligent Interaction*, 2024.
- [72] Torsten Wörtwein, Louis-Philippe Morency, and Stefan Scherer. Beyond additive fusion: Learning non-additive multimodal interactions. In *Findings of the Association for Computational Linguistics: EMNLP 2022*, 2022.
- [73] Dong Xiang, Sun-Yuan Hsieh, et al. G-good-neighbor diagnosability under the modified comparison model for multiprocessor systems. *Theoretical Computer Science*, 1028:115027, 2025.
- [74] Zihui Xue and Radu Marculescu. Dynamic multimodal fusion. In *Proceedings of the IEEE/CVF Conference on Computer Vision and Pattern Recognition Workshops*, 2023.
- [75] Zheyu Yao, Yichao Zhang, Ningyuan Deng, Xinyuan Song, Ziqian Bi, Keyu Chen, Ming Li, Qian Niu, Junyu Liu, Benji Peng, et al. Multimodal embeddings for representation learning. 2025.
- [76] Mingjie You, Kaijie Chen, and Dawei Cheng. Drdgrl: Dual-relational dynamic graph representation learning for delay-sensitive stock trend prediction. In *International Conference on Database Systems for Advanced Applications*, pages 35–50. Springer, 2026.
- [77] Haofei Yu, Zhengyang Qi, Lawrence Jang, Ruslan Salakhutdinov, Louis-Philippe Morency, and Paul Pu Liang. Mmoe: Enhancing multimodal models with mixtures of multimodal interaction experts. In *Proceedings of the 2024 Conference on Empirical Methods in Natural Language Processing*, pages 10006–10030, 2024.
- [78] Seniha Esen Yüksel, Joseph N. Wilson, and Paul D. Gader. Twenty years of mixture of experts. *IEEE Transactions on Neural Networks and Learning Systems*, 23(8):1177–1193, 2012.
- [79] Amir Zadeh, Rowan Zellers, Eli Pincus, and Louis-Philippe Morency. Mosi: Multimodal corpus of sentiment intensity and subjectivity analysis in online opinion videos. In *IEEE Intelligent Systems*, 2016.
- [80] AmirAli Bagher Zadeh, Paul Pu Liang, Soujanya Poria, Erik Cambria, and Louis-Philippe Morency. Multimodal language analysis in the wild: Cmu-mosei dataset and interpretable dynamic fusion graph. In *Proceedings of the 56th Annual Meeting of the Association for Computational Linguistics*, pages 2236–2246, 2018.
- [81] Danyang Zhang, Junhao Song, Ziqian Bi, Yingfang Yuan, Tianyang Wang, Joe Yeong, and Junfeng Hao. Mixture of experts in large language models. *arXiv:2507.11181*, 2025.
- [82] Haobo Zhang, Xutao Mao, Guangyuan Dong, Ziwei Li, Xuanbo Su, Kaijie Chen, Jing Yang, and Zheng Lin. Memmark: State-evolution attribution watermarking for agent long-term memory systems. *arXiv preprint arXiv:2605.25002*, 2026.
- [83] Yanfang Zhang, Shuo Zhang, and Kun Huang. Multimodal learning with missing modality: A survey. In *Proceedings of the 31st ACM International Conference on Multimedia*, 2023.
- [84] Qinjian Zhao, Zhihao Dou, Dinggen Zhang, Xiangyu Li, Chaoda Song, Zhongwei Wan, Xinpeng Li, Yanyan Zhang, Kaijie Chen, Qingtao Pan, et al. Stride: Strategic trajectory reasoning via discriminative estimation for verifiable reinforcement learning. *arXiv preprint arXiv:2606.15866*, 2026.
- [85] Weichao Zhao, Hao Feng, Qi Liu, Jingqun Tang, Binghong Wu, Lei Liao, Shu Wei, Yongjie Ye, Hao Liu, Wengang Zhou, et al. Tabpedia: Towards comprehensive visual table understanding with concept synergy. *Advances in Neural Information Processing Systems*, 37:7185–7212, 2025.

- [86] Zhen Zhao, Jingqun Tang, Chunhui Lin, Binghong Wu, Can Huang, Hao Liu, Xin Tan, Zhizhong Zhang, and Yuan Xie. Multi-modal in-context learning makes an ego-evolving scene text recognizer. In *Proceedings of the IEEE/CVF Conference on Computer Vision and Pattern Recognition*, pages 15567–15576, 2024.
- [87] Zhen Zhao, Jingqun Tang, Binghong Wu, Chunhui Lin, Shu Wei, Hao Liu, Xin Tan, Zhizhong Zhang, Can Huang, and Yuan Xie. Harmonizing visual text comprehension and generation. *arXiv preprint arXiv:2407.16364*, 2024.